Coupled Local Mode Method for Simulating Vibrational Spectroscopy

Matthew D. Hanson¹ and Steven A. Corcelli^{1, a)}
Department of Chemistry and Biochemistry, University of Notre Dame, Notre Dame, Indiana 46556, IISA

Experimental and theoretical studies have highlighted protonated water clusters (PWCs) as important models of the excess proton in aqueous systems. A significant focus has been characterizing the spectral signatures associated with different excess proton solvation motifs. Accurate vibrational frequency calculations are crucial for connecting the measured spectra to the structure of PWCs. In this paper, we extend and characterize a coupled local mode (CLM) approach for calculating the infrared spectra of PWCs, using the $H^+(H_2O)_4$ cluster as a benchmark system. The CLM method is relatively low cost and incorporates the anharmonicity and coupling of OH vibrations. Here, we demonstrate the accuracy of the technique compared to experiments. We also illustrate the dependence of calculated spectral features on the underlying electronic structure theory and basis sets used in the local mode frequency and coupling calculations.

I. INTRODUCTION

The study of aqueous solutions has drawn a significant amount of interest in the physical and chemical sciences. This is because aqueous environments are ubiquitous in biological, ecological, and chemical systems, which bear great importance across diverse scientific disciplines. It is particularly important to understand the structure and behavior of acidic and basic aqueous solutions, since they constitute the environment of many biological and ecological systems. For the hydrated proton, the solvation structure is typically characterized in relation to two extremes: (1) a symmetrically solvated hydronium species, H₃O⁺(H₂O)₃ or H⁺(H₂O)₄, called Eigen, and (2) a proton evenly shared by a pair of neighboring waters, $H_5O_2^+$ or $H^+(H_2O)_2$, called Zundel. ^{1,2} Unfortunately, despite extensive experimental and theoretical inquiry, the structure and dynamics of the hydrated excess proton remain controversial and demand further study.^{3–7}

Various techniques can be used to study aqueous systems, each suited uniquely to providing insights ranging from thermodynamic quantities to molecular structure and dynamics. In principle, infrared (IR) spectroscopy promises to identify the nature of the hydrated proton because of the sensitivity of the underlying molecular vibrations to their local chemical and solvation environments.^{8–10} Complicating the interpretation of the aqueous proton is the broad continuum spanning 1000 - 3000 cm⁻¹ in the IR absorption spectrum of acidic solutions. 4,6,11 This broad featureless region complicates the interpretation of the IR spectrum in terms of the limiting Eigen and Zundel species. 4-6 Attempting to disentangle these broad bands by examining the time-dependent 2D-IR responses has still not definitively resolved the interpretation of the IR spectra of aqueous acids.3,5,6 The continuum arises because the contributing vibrational modes are anharmonic and strongly coupled. Thus, minute structural fluctuations result in significant changes in vibrational frequencies that contribute to massive inhomogeneous broadening.^{8,12,13} In theoretical studies of the hydrated excess proton, it is thus critically important to utilize techniques that can capture both the anharmonicities in the vibrational potential energy surface (PES) and the in-

a)Electronic mail: scorcell@nd.edu

homogeneous broadening caused by fluctuations in the local chemical environment.

Concurrent with theoretical approaches that directly interrogate the structure of the aqueous hydrated proton are experimental techniques that aim to characterize the excess proton when it is isolated in a variety of simpler chemical motifs. Studies of cryogenic gas-phase protonated water clusters (PWCs), $H^+(H_2O)_n$, offer unique insights unavailable in the condensed phase. 14-17 For our purposes, PWCs offer an opportunity to directly probe the distinction between the Eigen and Zundel motifs; the Eigen and Zundel structures are essentially defined by the n = 4 and n = 2 clusters.^{1,2,18} Other clusters exhibit structures somewhere in between the limiting Eigen and Zundel motifs. 19,20 Both the Duncan and Johnson groups have extensively expanded the understanding of the hydrated excess proton by taking a bottom-up approach of studying PWCs of various sizes. 15,16,19-21 Because the clusters are cryogenically cooled, the IR spectra contain relatively distinct features amenable to interpretation in terms of specific vibrational modes associated with particular molecular structures, in contrast to the mostly featureless aqueous acid continuum. Johnson has used this approach to track the evolution of the excess proton's stretching modes throughout a variety of cluster sizes. 19,20

Johnson has also implemented an approach based on selective deuteration of the PWCs so that the spectral response given by modes on water molecules in distinct chemical environments can be isolated. 10,21,22 Selective deuteration is effective both because of the isotopic shift in the OH stretching and HOH bending frequencies caused by isotopic substitution of H with D, and the off-resonance modes are decoupled. 10,22 Both the $H^+(H_2O)_{21}$ and $Cs^+(H_2O)_{20}$ clusters have been studied using this selective deuteration approach. 10,22 These studies have provided enormous insights into the spectral responses caused by aqueous protons in different chemical environments.

The interpretation of the IR spectra of PWCs has benefited from theoretical studies. ^{21,23–26} The experimental spectra provide a benchmark of the accuracy of theoretical methods for computing vibrational frequencies and spectra. As in the condensed phase, the anharmonicity of the potential experienced by the excess proton prohibits the use of the harmonic approximation. Thus, harmonic normal mode calculations, which are standard in quantum chemistry packages, are unreliable

for PWCs.^{24,27} Moreover, the modes in PWCs are also anharmonically coupled, which leads to complicated mode mixing. For instance, the water stretching fundamental's accidental degeneracy with the bending overtone can lead to a Fermi resonance that significantly mixes the bending and stretching vibrations.^{23,27} Addressing these difficulties with PWCs will point towards new approaches for dealing with these same difficulties in the condensed phase.

Furthermore, high-level anharmonic vibrational structure methods have been applied to PWCs. The Meyer group used the multiconfiguration time-dependent Hartree (MCTDH) method to perform a full-dimensional (15 dimensions) quantum-dynamical calculation on the Zundel molecule, H₅O₂⁺. ^{1,18} The Bowman group has used the VSCF/VCI method implemented in the MULTIMODE software package to study PWCs, including the three-dimensional $H^+(H_2O)_{21}$ cluster. 28-30 Spectra produced with these methods give impressive quantitative agreement with experiment. Unfortunately, the computational cost of these methods makes them relatively difficult to apply to problems in the condensed phase. The high-level calculations on PWCs have generally used an *ab initio* many-body PES and dipole moment surface (DMS) to reduce computational costs. ^{31,32} These PESs/DMSs are, however, generally quite costly to obtain if a high-level of electronic structure theory is utilized.³³ The VSCF/VCI calculations performed by Bowman have also sometimes used a local monomer approximation to separate the vibrations of the cluster into modes on several individual water molecules and the solvated Eigen or Zundel species. 28,34

A subset of different studies have combined sampling unique structures from molecular dynamics (MD) simulations and calculating the vibrational frequencies using density functional theory (DFT) and discrete variable representation (DVR) of OH stretches in acidic and basic aqueous condensed-phase solutions. 4,8,35,36 Others have used the Fourier transform of the dipole autocorrelation function to generate the IR spectrum.^{8,37} The choice of methods used to generate the MD trajectories of both aqueous systems and certain PWCs varies from purely classical force-field simulations to quantum ring-polymer MD simulations. 4,8,23,38,39 In several instances, the vibrational frequencies computed using DFT were used to develop empirical frequency maps. 40 This simplifies the calculation of the OH stretch vibrational frequency of interest to computing collective variables that are available from the MD simulations.^{8,35} For instance, the electric field along the OH bond can be used to create a map of the frequency and transition dipole moment vector magnitudes.^{8,35} The vibrational frequency map-based methods have given insight into the IR spectra of water and aqueous solutions in the condensed phase. They have not, however, been applied to gas-phase PWCs where comparison can be made to the relatively isolated spectral features in the experiment and other high-level methods, which invites an avenue of further study.

In this paper, we extend and validate the coupled local mode (CLM) approach for calculating the IR spectra of PWCs, though it can be applied to other systems as well.²⁶ The CLM method proceeds in a series of steps. First, snapshots of the cluster are sampled from an *ab initio* molecu-

lar dynamics simulation. For each of these snapshots, a series of local modes (LMs) are generated from numerically solving the Schrödinger equation using a generalization of Miller's discrete variable representation (DVR) method and evaluating the differences between the eigenvalues of the LM Hamiltonians. 41,42 Bi-linear coupling constants are then calculated for each pair of local modes. Finally, the LMs are coupled, and the resultant coupled modes are used to generate an inhomogeneous IR spectrum that is deconvoluted in terms of the participating LMs. This method produces a reasonably cost-effective and accurate approach which has the versatility to be applied in the condensed phase. As a benchmark of this method, we will primarily study the Eigen cluster, $H^+(H_2O)_4$. We have recently shown several results for more complex clusters using the CLM method, but here we present the theoretical basis for the CLM method in more detail.²⁶ A detailed analysis of the sensitivity of the CLM method to various choices in electronic structure and derivative expansion are also presented. Finally, we show that several reasonable cost-reduction schemes can be applied to utilize the CLM method for more complex systems.

II. COUPLED LOCAL MODE VIBRATION THEORY

A. The Approxmate Vibrational Hamiltonian

We begin with Wilson's form of the vibrational Hamiltonian written in terms of the internal coordinates $\{q_i\}$, ⁴³

$$\hat{H} = -\frac{\hbar^2}{2} \sum_{i,k}^{M} \left[\frac{\partial}{\partial q_i} g^{jk} \frac{\partial}{\partial q_k} \right] + \hat{V}(\{q_j\}) \tag{1}$$

where g^{jk} are Wilson's G matrix elements. ⁴³ In order to utilize this Hamiltonian, the potential energy is expanded using a multidimensional Taylor series in up to two of the M internal coordinates that are chosen to be treated quantum mechanically. For the purposes of this paper, these will be the OH bond lengths and HOH bending angles. The expansion is truncated at two coordinates so that only vibrational couplings between pairs of LMs are considered. The Taylor expansion is performed at a point where each internal coordinate that is treated quantum mechanically is at its equilibrium value in the sampled geometry, denoted by the subscript label P. Note that this is not the same as an equilibrium geometry, since other coordinates are not necessarily at their equilibrium value. Thus, thermal fluctuations away from equilibrium are intrinsically incorporated into the CLM calculations. This expansion gives,

$$\begin{split} \hat{V}(\{q_j\}) = & \sum_{n_1=0}^{\infty} \cdots \sum_{n_M=0}^{\infty} \left[\prod_{k=1}^{M} \frac{\left(\hat{q}_k - q_{k,eq}\right)^{n_k}}{n_k!} \right] \left(\frac{\partial^{\sum_k^M n_k V}}{\prod_k^M \partial q_k^{n_k}} \right)_P \\ \approx & \sum_{j}^{M} \sum_{m=0}^{\infty} \frac{\delta \hat{q}_j^m}{m!} \left(\frac{\partial^m V}{\partial q_j^m} \right)_P \\ & + \sum_{j>k}^{M} \sum_{m,n=1}^{\infty} \frac{\delta \hat{q}_j^m \delta \hat{q}_k^n}{m!n!} \left(\frac{\partial^{m+n} V}{\partial q_j^m \partial q_k^n} \right)_P \end{split}$$

$$\approx \sum_{j}^{M} V(q_{j}) + \sum_{j>k}^{M} \sum_{m,n=1}^{\infty} \frac{\delta \hat{q}_{j}^{m} \delta \hat{q}_{k}^{n}}{m! n!} \left(\frac{\partial^{m+n} V}{\partial q_{j}^{m} \partial q_{k}^{n}} \right)_{P}$$
 (2)

where $\delta \hat{q}_j^m \equiv (\hat{q}_j - q_{j,eq})^m$, $q_{j,eq}$ is the equilibrium value of q_j , and single coordinate derivatives of all orders have been combined into smooth functions $V(q_j)$. The vibrational Hamiltonian in equation (1) now consists of a sum of diagonal and off-diagonal operators in terms of the internal coordinates.

Next, the vibrational Hamiltonian in equation (1) is partitioned into a set of local and coupling operators,

$$\hat{H} = \hat{H}_{local} + \hat{H}_{coup}$$

$$\hat{H}_{local} \equiv \sum_{j}^{M} \hat{H}(q_{j})$$

$$\equiv \sum_{j} \left[-\frac{\hbar^{2}}{2} \frac{\partial}{\partial q_{j}} g^{jj} \frac{\partial}{\partial q_{j}} + \hat{V}(q_{j}) \right]$$

$$= \sum_{j} \left[-\frac{\hbar^{2}}{2} \frac{\partial g^{jj}}{\partial q_{j}} \frac{\partial}{\partial q_{j}} - \frac{\hbar^{2}}{2} g^{jj} \frac{\partial^{2}}{\partial q_{j}^{2}} + \hat{V}(q_{j}) \right]$$

$$\hat{H}_{coup} \approx \sum_{j>k}^{M} \hat{H}(q_{j}, q_{k})$$

$$\equiv \sum_{j>k}^{M} \left[-\frac{\hbar^{2}}{2} \frac{\partial}{\partial q_{j}} g^{jk} \frac{\partial}{\partial q_{k}} - \frac{\hbar^{2}}{2} \frac{\partial}{\partial q_{k}} g^{jk} \frac{\partial}{\partial q_{j}} \right]$$

$$+ \sum_{j>k}^{M} \sum_{m,n=1}^{\infty} \frac{\delta \hat{q}_{j}^{m} \delta \hat{q}_{k}^{n}}{m! n!} \left(\frac{\partial^{m+n} V}{\partial q_{j}^{m} \partial q_{k}^{n}} \right)_{P}$$

$$= \sum_{j>k}^{M} \left[-\frac{\hbar^{2}}{2} \frac{\partial g^{jk}}{\partial q_{j}} \frac{\partial}{\partial q_{k}} - \frac{\hbar^{2}}{2} \frac{\partial g^{jk}}{\partial q_{k}} \frac{\partial}{\partial q_{j}} - \hbar^{2} g^{jk} \frac{\partial^{2}}{\partial q_{j} \partial q_{k}} \right]$$

$$+ \sum_{j>k}^{M} \sum_{m,n=1}^{\infty} \frac{\delta \hat{q}_{j}^{m} \delta \hat{q}_{k}^{n}}{m! n!} \left(\frac{\partial^{m+n} V}{\partial q_{j}^{m} \partial q_{k}^{n}} \right)_{P}$$
(5)

where $\hat{H}(q_j)$ is interpreted as the Hamiltonian operator associated to the motion along an internal coordinate q_j , and $\hat{H}(q_j, q_k)$ denotes the Hamiltonian operator corresponding to the coupling between motions along coordinates q_j and q_k .

B. The CLM Representation

In order to solve for the coupled mode transition frequencies, a representation of the vibrational Hamiltonian in a LM basis is constructed. The LM approximation consists of treating the eigenfunctions of \hat{H}_{local} as separable in terms of excitations involving the individual internal coordinates.⁴⁴ Equivalently, this approximation is equivalent to a separation of variables, as implied by equation (4). The eigenstates of \hat{H}_{local} are then given by the product of the eigenstates of each single-coordinate Hamiltonian from equation (4),⁴⁵

$$\hat{H}(q_j) \left| \psi_{n_1}^1 \psi_{n_2}^2 \cdots \psi_{n_j}^j \cdots \right\rangle = \varepsilon_{n_j}^j \left| \psi_{n_1}^1 \psi_{n_2}^2 \cdots \psi_{n_j}^j \cdots \right\rangle$$
 (6)

$$\hat{H}_{local} \left| \psi_{n_1}^1 \psi_{n_2}^2 \cdots \right\rangle = \left[\sum_{j} \varepsilon_{n_j}^j \right] \left| \psi_{n_1}^1 \psi_{n_2}^2 \cdots \right\rangle \tag{7}$$

where n_j is the number of quanta associated with coordinate q_j , and $\mathcal{E}_{n_j}^j$ is the corresponding energy contribution. Note that equation (6) implies that each LM Hamiltonian, $\hat{H}(q_j)$, only acts on its own wavefunctions. In this paper, we will focus on states with quanta in only one coordinate, which admits a simplifying notation,

$$\left|\psi_{n_j}^{(j)}\right\rangle \equiv \left|\psi_0^1 \cdots \psi_0^{j-1} \psi_{n_j}^j \psi_0^{j+1} \cdots\right\rangle \tag{8}$$

This forms an orthogonal basis to construct a representation of the vibrational Hamiltonian. The matrix elements of \hat{H}_{local} from equation (4) with respect to the one-mode product states in equation (8) are thus given by,

$$\left\langle \psi_{n_j}^{(j)} \middle| \hat{H}_{local} \middle| \psi_{n_k}^{(k)} \right\rangle = \left(\varepsilon_{n_j}^j + \sum_{l \neq j} \varepsilon_0^l \right) \delta_{n_j n_k} \delta_{jk}$$
 (9)

This means the ground state transition frequency associated with a given LM can be evaluated as,

$$\omega_{n_{j}0}^{j} \equiv \frac{\left\langle \psi_{n_{j}}^{(j)} \middle| \hat{H}_{local} \middle| \psi_{n_{j}}^{(j)} \right\rangle - \left\langle 0 \middle| \hat{H}_{local} \middle| 0 \right\rangle}{\hbar}$$

$$= \frac{\varepsilon_{n_{j}}^{j} - \varepsilon_{0}^{j}}{\hbar}$$
(10)

where $|0\rangle$ is the ground state with no quanta in any modes. In other words, to evaluate the LM transition frequencies all that is needed are the excitation energies for individual internal coordinates. The diagonal elements of the CLM representation of the Hamiltonian in equation (3) are thus written as,

$$\left\langle \psi_{n_j}^{(j)} \middle| \hat{H}(q_j) \middle| \psi_{n_k}^{(k)} \right\rangle = \varepsilon_{n_j}^j \delta_{n_j n_k} \delta_{jk}$$
 (11)

since the states in equation (8) only involve excitation of a single coordinate.

The coupled local modes (CLMs) are obtained by coupling the LM transitions via the appropriate matrix elements from \hat{H}_{coup} in equation (5).^{8,44} The couplings between the LMs associated to q_j and q_k have matrix elements of the form,

$$\left\langle \psi_{n_{j}}^{(j)} \middle| \hat{H}(q_{j}, q_{k}) \middle| \psi_{n_{k}}^{(k)} \right\rangle = \left\langle \psi_{n_{j}}^{(j)} \middle| - \frac{\hbar^{2}}{2} \frac{\partial g^{jk}}{\partial q_{j}} \frac{\partial}{\partial q_{k}} - \frac{\hbar^{2}}{2} \frac{\partial g^{jk}}{\partial q_{k}} \frac{\partial}{\partial q_{j}} - \hbar^{2} g^{jk} \frac{\partial^{2}}{\partial q_{j} \partial q_{k}} \middle| \psi_{n_{k}}^{(k)} \right\rangle
+ \sum_{j,k}^{M} \sum_{m,n=1}^{\infty} \frac{\left\langle \psi_{n_{j}}^{(j)} \middle| \delta \hat{q}_{j}^{m} \delta \hat{q}_{k}^{n} \middle| \psi_{n_{k}}^{(k)} \right\rangle}{m! n!} \left(\frac{\partial^{m+n} V}{\partial q_{j}^{m} \partial q_{k}^{n}} \right)_{P}
= \left\langle \psi_{n_{j}}^{(j)} \middle| - \frac{\hbar^{2}}{2} \frac{\partial g^{jk}}{\partial q_{j}} \frac{\partial}{\partial q_{k}} - \hbar^{2} g^{jk} \frac{\partial^{2}}{\partial q_{j} \partial q_{k}} \middle| \psi_{n_{k}}^{(k)} \right\rangle
+ \sum_{m,n=1}^{\infty} \frac{\left[\delta \hat{q}_{j}^{m} \middle|_{n_{j}0} \left[\delta \hat{q}_{k}^{n} \middle|_{0n_{k}} \left(\frac{\partial^{m+n} V}{\partial q_{j}^{m} \partial q_{k}^{n}} \right)_{P} \right] (12)$$

where in the second step the matrix elements of the potential are simplified and the product rule has been used. Evaluating the derivatives is done with the general finite difference formula for a function f(x,y),

$$\left(\frac{\partial^{n+m} f}{\partial x^n \partial y^m}\right)_{x_0, y_0} \approx \frac{1}{2^{n+m} h_x^n h_y^m} \sum_{k=0}^n \sum_{l=0}^m \left[(-1)^{k+l} \binom{n}{k} \binom{m}{l} \right] \times f(x_0 + [n-2k]h_x, y_0 + [m-2l]h_y) \tag{13}$$

where $\binom{n}{k}$ is a binomial coefficient and h_x and h_y are the finite difference steps along the coordinates x and y, respectively. ⁴⁶ In practice, the infinite series expansion of the potential is truncated with a very small number of terms.

After calculating the local modes and couplings, or diagonal and off-diagonal matrix elements, in equations (11) and (12), the CLM representation of the vibrational Hamiltonian in equation (3) is constructed from its matrix elements, which is denoted **H**. This effective representation of the vibrational Hamiltonian allows for the determination of the coupled mode transition frequencies and their contributions in terms of the local mode frequencies.

C. Coupled Mode Frequencies and Intensities

The CLM Hamiltonian matrix \mathbf{H} can be diagonalized to give the coupled energies and mixed states, represented by the equation $\mathbf{H} = \mathbf{B}\mathbf{E}\mathbf{B}^T$, where \mathbf{E} is the diagonal matrix of coupled energies and the columns of \mathbf{B} contain the coefficients giving the contribution of the basis states in equation (6) to the coupled energy states, including $|0\rangle$. The ground state is not coupled to the other (off-resonance) states in the CLM method. Thus, the expansion $\mathbf{H} = \mathbf{E}_0 \oplus \mathbf{H}'$ is warranted, where \mathbf{H}' is the CLM Hamiltonian excluding the ground state, \oplus is the matrix direct sum, and,

$$E_0 \equiv \sum_{i} \varepsilon_0^j \tag{14}$$

This also gives,

$$\mathbf{H} = (1 \oplus \mathbf{B}')(\mathbf{E}_0 \oplus \mathbf{E}')(1 \oplus \mathbf{B}')^{\mathrm{T}}$$
 (15)

where the connection between both E, B and E', B' is the same as the relation between H and H'. The transition frequency and coupling matrix κ , whose diagonal elements are the LM transition frequencies and whose off-diagonal elements are the couplings between them, can thus be defined,

$$\kappa \equiv \frac{\mathbf{H}' - E_0 \mathbf{I}}{\hbar}$$

$$= \mathbf{B}' \mathbf{\Omega} \mathbf{B}'^T$$
(16)

where **I** is the identity matrix, Ω is the diagonal matrix of coupled transition frequencies ω_i^C , and in the second step κ has

been diagonalized. This means that the coefficients in a column of ${\bf B}'$ are interpreted as the contributions of a given LM to the CLM whose transition frequency is given by the appropriate eigenvalue via $\omega_j^C \equiv (E_j'-E_0)/\hbar$. The construction of κ means that the LM energies are not needed to obtain the CLM transition frequencies, since the coupled transitions can be constructed from only the LM transition frequencies.

From this analysis, the transition dipole moment (TDM) for a given CLM can also be written in terms of the LM TDMs. This can be justified by writing the dipole moment operator as a Taylor expansion in the internal coordinates about their equilibria in the sampled geometry in a manner similar to the treatment of the potential energy in equation (2),

$$\vec{\mu} = \sum_{n_1=0}^{\infty} \cdots \sum_{n_M=0}^{\infty} \left[\prod_{k=1}^{M} \frac{\left(\hat{q}_k - q_{k,eq}\right)^{n_k}}{n_k!} \right] \left(\frac{\partial^{\sum_k^M n_k} \vec{\mu}}{\prod_k^M \partial q_k^{n_k}} \right)_{eq}$$

$$\approx \sum_{j=0}^{M} \sum_{m=0}^{\infty} \frac{\delta \hat{q}_j^m}{m!} \left(\frac{\partial^m \vec{\mu}}{\partial q_j^m} \right)_{eq} + \cdots$$

$$\equiv \sum_{j=0}^{M} \vec{\mu}(q_j)$$
(17)

where the exclusion of the derivatives in more than one internal coordinate is motivated by the fact that $\langle 0|\delta\hat{q}_j|0\rangle\approx 0$, as this state is relatively harmonic, and terms involving higher powers of $\delta\hat{q}_j$ are likewise small. Equation (17) allows the TDM between the ground state and a coupled state to be written as,

$$\vec{\mu}_{j}^{C} = \sum_{k} B'_{kj} \left\langle \psi^{(k)} \middle| \vec{\mu} \middle| 0 \right\rangle$$

$$= \sum_{k} B'_{kj} \left\langle \psi^{(k)} \middle| \sum_{l} \vec{\mu}(q_{l}) \middle| 0 \right\rangle$$

$$= \sum_{k} B'_{kj} \left\langle \psi^{k} \middle| \vec{\mu}(q_{k}) \middle| 0 \right\rangle$$

$$\equiv \sum_{k} B'_{kj} \vec{\mu}_{T}^{k}$$
(18)

where the number of quanta in the state $\langle \psi^{(k)} |$ is left ambiguous so that the index k can refer to different numbers of quanta in the same coordinate, if necessary, and the notation $\vec{\mu}_T^k \equiv \langle \psi^k | \vec{\mu}(q_k) | 0 \rangle$ has been defined to deal with the ambiguity of how many quanta are in the LM TDM. The LM TDM for a specific number of quanta, $\vec{\mu}_{k0}^j$, has the usual interpretation,

$$\vec{\mu}_{k0}^{j} \equiv \int_{D} dq_{j} \psi_{k}^{j*}(q_{j}) \hat{\mu} \psi_{0}^{j}(q_{j}) \tag{19}$$

in which D is the appropriate domain for the internal coordinate of interest. LM TDMs are calculated using the DVR wavefunctions. The intensity of the normal mode transition ω_j^C is thus given by $I(\omega_j^C) \propto |\vec{\mu}_j^C|^2$, in accord with Fermi's Golden Rule. ^{48,49} In order to deal with combination bands, terms involving the relevant pairs of coordinates must be included in the expansion, though this will not be addressed in this paper.

D. Generalized DVR Method

In order to compute the LM wavefunctions and energies, we have developed a generalization of Colbert and Miller's DVR approach to the solution of differential equations. ^{41,42,50} A complete description of our derivation is given in the Supple-

mentary Material (SM). This approach allows an analytic Hermitian representation of any differential operator up to second order differentials, making the representation of the Hamiltonian matrix particularly simple. For a given set of N-1 grid points $\{x_{\alpha}=a+\alpha\Delta x:\alpha\in[1,N-1]\}$ on the domain [a,b] with uniform spacing $\Delta x\equiv\frac{b-a}{N}$, we obtain the formulas,

$$[f(x)]_{\alpha\beta}^{DVR} = \left[\frac{f(x_{\alpha}) + f^*(x_{\beta})}{2} \right] \delta_{\alpha\beta}$$
 (20)

$$\left[f(x)\frac{\partial}{\partial x}\right]_{\alpha\beta}^{DVR} = -\frac{\pi(-1)^{\alpha-\beta}}{4N\Delta x} \begin{cases} \frac{\left[f^*(x_{\alpha}) + f(x_{\alpha})\right]}{\tan\left(\frac{\pi\alpha}{N}\right)} & \alpha = \beta \\ \frac{\left[f^*(x_{\beta}) - f(x_{\alpha})\right]}{\tan\left(\frac{\pi(\alpha-\beta)}{2N}\right)} + \frac{\left[f^*(x_{\beta}) + f(x_{\alpha})\right]}{\tan\left(\frac{\pi(\alpha+\beta)}{2N}\right)} & \alpha \neq \beta \end{cases}$$
(21)

$$\left[f(x)\frac{\partial^{2}}{\partial x^{2}}\right]_{\alpha\beta}^{DVR} = -\frac{\pi^{2}(-1)^{\alpha-\beta}}{4N^{2}\Delta x^{2}} \begin{cases}
\left[f(x_{\alpha}) + f^{*}(x_{\alpha})\right] \left[\frac{2N^{2}+1}{3} - \frac{1}{\sin^{2}\left(\frac{\pi\alpha}{N}\right)}\right] & \alpha = \beta \\
\frac{f(x_{\alpha}) + f^{*}(x_{\beta})}{\sin^{2}\left(\frac{\pi(\alpha-\beta)}{2N}\right)} - \frac{f(x_{\alpha}) + f^{*}(x_{\beta})}{\sin^{2}\left(\frac{\pi(\alpha+\beta)}{2N}\right)} & \alpha \neq \beta
\end{cases} \tag{22}$$

where f(x) is a well-behaved function with a Taylor expansion. Note that equation (20) implies that the LM potential operator is represented by a diagonal matrix of potentials evaluated at the grid points for a given internal coordinate. Equations (20), (21) and (22) apply to coordinates x of any type on any domain. In the infinite limits and for appropriate choices of f(x), these reproduce Colbert and Miller's results. An example of the DVR approach for a stretching coordinate of $H^+(H_2O)_4$ is given in Figure 1. Matrix elements of operators using the DVR wavefunctions $\{\psi_k\}$, such as the LM TDM in equation (19), are given by the formula for generic \hat{A} ,

$$\langle \psi_k | \hat{A} | \psi_l \rangle = \sum_{\alpha, \beta = 1}^{N-1} \psi_k^*(x_\alpha) A_{\alpha\beta}^{DVR} \psi_l(x_\beta) \Delta x \qquad (23)$$

III. SIMULATION AND CALCULATION DETAILS

The same AIMD simulation that was used in our previous study of PWCs was utilized for this paper.²⁶ We repeat the details of the simulation here for completeness. A Born-Oppenheimer AIMD simulation of the H⁺(H₂O)₄ cluster was performed using the CP2K open-source software package with a time step of 0.5 fs and the BLYP exchange-correlation functional with Grimme's D3 correction.^{39,51,52} CP2K uses the Quickstep method for force evaluations with the Gaussian and plane waves scheme.⁵³ A TZVP-GTH basis set was employed in the AIMD simulation, where the core electrons are described with Goedecker-Teter-Hutter (GTH)

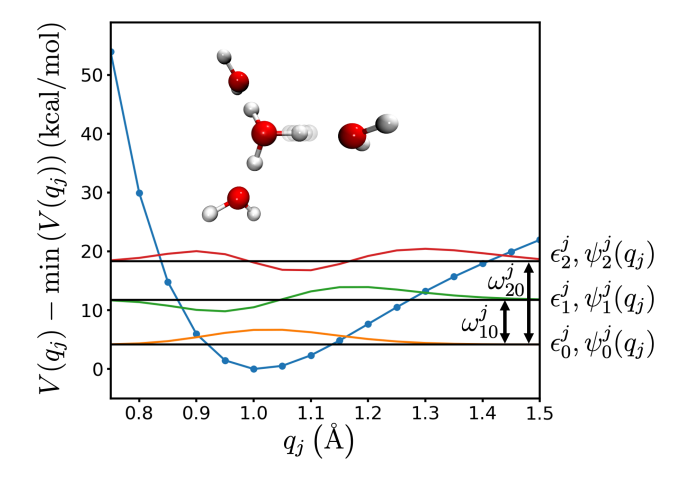


FIG. 1: Example of the DVR approach where q_j is a stretching coordinate of the hydronium core of $\mathrm{H^+(H_2O)_4}$ visualized in the inset. The first three energy levels and wavefunctions obtained from the DVR approach are shown and labeled.

pseudopotentials.⁵⁴ The simulation of $H^+(H_2O)_4$ was performed in the NVT ensemble with a canonical sampling through velocity rescaling (CSVR) thermostat with a time constant of 100 fs to constrain the temperature at 77 K.⁵⁵ The starting point for the simulation was an optimized structure, which was equilibrated for 10 ps. The production run of 500 ps generated 2000 snapshots spaced by 250 fs for further analysis.

Unless otherwise stated, the PES for every OH stretch and HOH bend LM in each of the sampled snapshots was computed using the designated electronic structure method and the 6-311G++(d, p) basis set in the Q-Chem software package.⁵⁶ OH stretch potential energy curves used 16 DVR grid points in the domain [0.75 Å, 1.5 Å] with 0.05 Å increments, and HOH bend potential energy curves used 18 grid points in the domain [70°, 155°] with 5° increments.

Coupling calculations are truncated at the first order derivative in the potential for the stretch-stretch fundamental couplings and at third order derivatives for the stretch fundamental-bend overtone couplings, since these couplings are an intrinsically anharmonic effect. Analysis of the fitness of these truncations is shown in the SM. Finite difference steps of $h_r = 0.02$ Å were used for the stretches and $h_\theta = 2^\circ$ for the bends, which were found to provide converged values of the derivatives.

All necessary equations for the Wilson G matrix elements, the local mode and coupling operators, and the matrix elements for the couplings are given in our previous paper. Examples of the DVRs taken from our general equations (20), (21), and (22) of various operators are also shown in this prior work. The method for the spectral deconvolution of the CLM IR spectra is also the same as in our previous paper. ²⁶

IV. RESULTS AND DISCUSSION

In order to benchmark the sensitivity of our CLM method to choices in electronic structure calculations, we simulated the IR spectrum of $H^+(H_2O)_4$ using the same AIMD trajectory and corresponding 2000 snapshots while employing different electronic structure methods for the calculations required in each spectrum. In Figure 2 we present the results of three DFT methods compared with experimental results from Johnson and coworkers, and in Figure 3 we present the CLM results of three different wavefunction-based electronic structure methods. Although systematic differences in the cal-

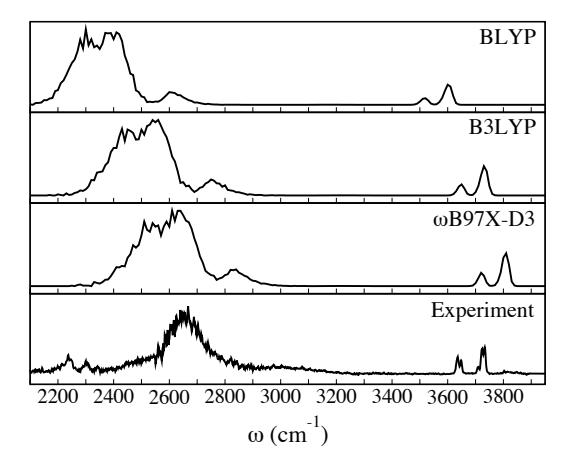


FIG. 2: Comparison of IR CLM spectra calculated using DFT-based electronic structure methods and experiment.

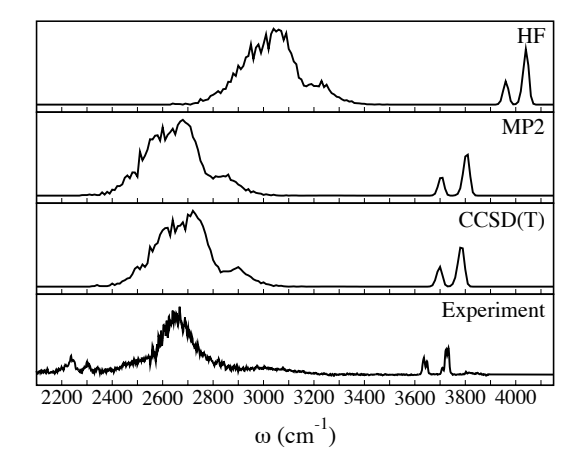


FIG. 3: Comparison of IR CLM spectra calculated using wavefunction-based electronic structure methods and experiment.

culated frequencies across different electronic structure methods could be found for water molecules in distinct chemical environments, each method reliably produced the same pattern of peaks with comparable intensity profiles. This suggests the discrepancies are more related to the underlying electronic structure rather than from approximations in the CLM methodology. Although the CCSD(T) and MP2 results are the most accurate, their computational cost exceeds the DFT methods, especially for CCSD(T).

The DFT spectral shapes are qualitatively identical to the CCSD(T) results, but the peak locations are not as precisely matched to experiment for the modes associated to the H₃O⁺ core. The calculated linewidth of the prominent H₃O⁺ feature around 2600 cm⁻¹ originates from inhomogeneous effects (i.e., from different structures sampled from the AIMD simulations). Previous VSCF/VCI calculations identified combination bands between the H₃O⁺ stretches and lower frequency hindered rotation and wagging motions, which also contribute to the linewidths, but are absent in this work.³⁰ However, the VSCF/VCI calculations neglect inhomogeneous effects, and both the CLM and VSCF/VCI approaches ignore dynamical and population lifetime effects.⁸ Thus, further investigations are required to have a satisfactory understanding of the H₃O⁺ linewidth. Nevertheless, the savings in computational cost make DFT a viable method for most applications, and we will discuss a correction approach below. Note, we also examined the extent to which the D3 correction affects the frequencies by directly comparing B3LYP and B3LYP-D3 calculations of the OH stretch LM frequencies of 300 H⁺(H₂O)₄ snapshots (Figure SM.4). The RMS difference in the calculated frequencies is 2.46 cm⁻¹, indicating the D3 correction does not have a substantial effect on the frequency calculations.

We have also studied the effects of varying the basis set size on the IR CLM spectra systematically to determine what constitutes sufficient convergence with respect to basis set size. We chose to study a set of double, triple, and quadruple zeta Dunning-style basis sets all using the B3LYP DFT method for $H^+(H_2O)_4$. As shown in Figure 4, there is no substantial

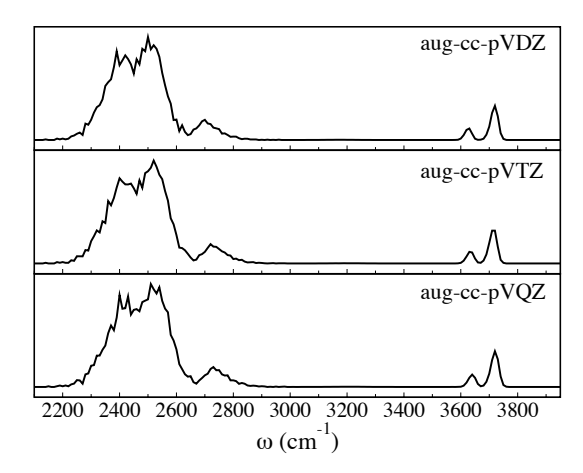


FIG. 4: Comparison of IR CLM spectra calculated using B3LYP electronic structure method with varying Dunning-style basis sets.

difference between the spectra calculated using these different basis sets, meaning that the vibrational frequencies are reasonably well converged at even the aug-cc-pVDZ level (roughly comparable to the 6-311G++(d,p) basis set used in our previous study).²⁶

Next, we consider several methods to incorporate higher-level calculations of the LMs and couplings without incurring excess cost. First, we consider mapping electronic structure results obtained from calculations at a lower level of electronic structure to those obtained at a higher level. For instance, in Figure 5 we show the results of fitting a subset of stretching LM frequencies obtained at the B3LYP level with the same frequencies obtained at the CCSD(T) level. The strength of this fit implies that a small subset of LM data obtained at higher levels of theory can be used to correct the lower-level results to save on computational costs.

A similar fitting procedure for the couplings can be used to relate the couplings calculated with a lower order truncation of the potential energy expansion to those calculated at a higher order truncation. A comparison of couplings obtained by truncating the expansion at 2^{nd} order derivatives, 3^{rd} order derivatives, and 4th order derivatives is shown in the SM. Likewise, we also show a fit between couplings calculated using DFT and higher level methods. Interestingly, the corrections to the coupling expansion and the level of electronic structure theory almost entirely cancel out (yielding $\approx 98\%$ of the uncorrected DFT value), meaning that DFT can be used to obtain surprisingly accurate stretch-stretch couplings without correction.

Finally, we evaluate the Förster dipole-dipole description of the couplings between stretches on adjacent molecules. In the Förster picture, the stretch-stretch couplings arise solely from the interactions of the transition dipole moments on OH stretching chromophores, yielding a formula for the interaction, ^{8,57}

$$\omega_F^{jk} = \vec{\mu}_{10}^j \cdot \vec{\mu}_{10}^k \left(\frac{\hat{r}_{OH}^j \cdot \hat{r}_{OH}^k - 3(\hat{r}_{OH}^j \cdot \hat{n}_{jk})(\hat{r}_{OH}^k \cdot \hat{n}_{jk})}{r_{jk}^3} \right)$$
(24)

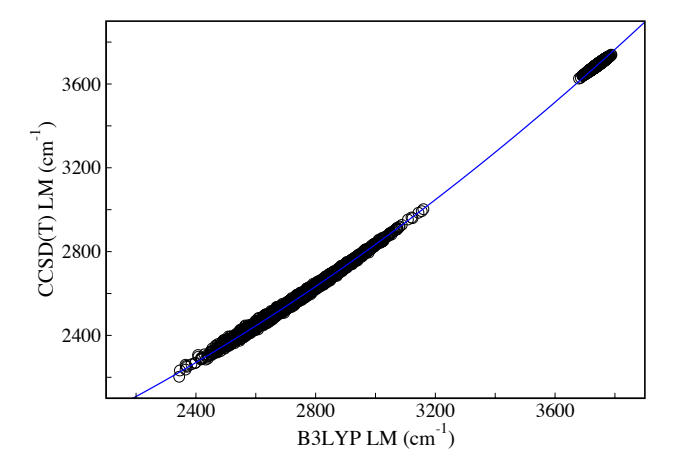


FIG. 5: Plot of the *ab initio* 1-0 stretching local modes of $\mathrm{H^+(H_2O)_4}$ calculated at the CCSD(T)/6-311G++(d,p) level, ω_{CC} , against the modes calculated from the same snapshots at the B3LYP/6-311G++(d,p) level, ω_{DFT} . The blue curve is the best fit of over 18,000 local modes given by the equation $\omega_{CC} \approx 0.00016 \omega_{DFT}^2 + 0.07517 \omega_{DFT} + 1168.03$ with an r^2 of 0.9999.

where \hat{r}_{OH}^{j} is the unit vector corresponding to OH bond with index j, \hat{n}_{jk} is the unit vector stretching from dipole j to dipole k, and r_{ik} is the distance between the dipole moment vectors. Skinner's convention of placing the dipole moments 58% of the way along the bond stretching vectors will be adopted for simplicity.⁸ Because only the TDMs calculated using the DVR approach are needed, this leads to a dramatic reduction of cost when calculating the couplings. The results of fitting intermolecular couplings calculated at the B3LYP/6-311G++(d,p) level of electronic structure theory to the Förster approximation of the couplings is given in Figure 6. Clearly, the Förster couplings can be reasonably used to approximate the couplings if a sufficient fit is performed. The group of coupling constants near zero are for pairs of OH stretches separated by larger distances and whose relative orientation is somewhat random. The other collection with larger magnitudes and negative sign is between OH groups on neighboring water or hydronium molecules, which are closer together and are in a more well-defined relative orientation. As expected, the Förster dipole-dipole model is more accurate for computing the coupling constant of more distal OH stretches. Interestingly, a comparable fit can be made between the Förster couplings and the potential energy portion of the intramolecular couplings, despite the Förster formula vastly overestimating the coupling strength. This result is shown in the SM.

V. CONCLUDING REMARKS

In this paper, we have shown the theoretical details of the CLM method for the calculation of vibrational spectra and have applied it to the IR spectrum of the benchmark $\mathrm{H^+(H_2O)_4}$ cluster. We also showed a generalization of Miller's DVR scheme for solving linear differential equations

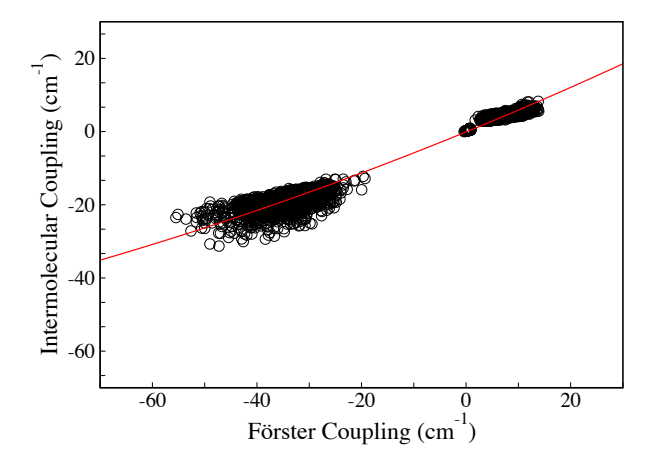


FIG. 6: Plot of the *ab initio* uncorrected $2^{\rm nd}$ order intermolecular stretch-stretch couplings ω_e^{jk} of H⁺(H₂O)₄ against the Förster couplings. The red curve is the best fit of over 6000 couplings given by the equation $\omega_e^{jk} \approx 0.0012 \left(\omega_F^{jk}\right)^2 + 0.5844 \omega_F^{jk} - 0.097$ with an r^2 of 0.98.

and calculating matrix elements. The consistency of broad spectral features for a variety of different electronic structure methods was established, though the location of the distinct features was shown to change depending upon the method chosen. The dependence of the calculated vibrational couplings on the order of the PES expansion and the electronic structure method was shown to be relatively modest, and it was further shown that 2nd order B3LYP couplings are surprisingly accurate due to a fortuitous cancellation of error. Finally, it was shown that accurate fits between the local modes calculated at lower and higher levels of electronic structure theory could be used to increase accuracy with modest cost. It was also shown that the couplings could be approximated with simple electrostatic models, such as the Förster dipole-dipole coupling model for the stretch-stretch couplings. This leads to a drastic reduction in the number of calculations needed in the CLM method, particularly for larger systems. Thus, the prospects of applying the CLM method to aqueous acid, base, and salt solutions in the condensed phase are promising, including the calculation of two-dimensional infrared (2D IR) spectra. Presently, we are restricted to the OH stretch, HOH bend, and OH stretch-HOH bend overtone manifold. However, these are the features that dominate aqueous condensed phase vibrational spectra above 1500 cm⁻¹. Nevertheless, including the effects of lower frequency combination bands is a critical challenge for future methodological work.

SUPPLEMENTARY MATERIAL

The Supplementary Material contains a full derivation of the generalized Miller DVR formulas, an analysis of the truncation of the derivative expansion and electronic structure methods for the vibrational couplings, an analysis of the Förster approximation for the intramolecular couplings, and analysis of the D3 correction's effect on the local mode frequencies.

ACKNOWLEDGMENTS

This work was supported by the National Science Foundation (CHE-2154552). The authors are grateful for computing resources and support at the Center for Research Computing at the University of Notre Dame.

¹O. Vendrell, F. Gatti, D. Lauvergnat, and H.-D. Meyer, "Full-dimensional (15-dimensional) quantum- dynamical simulation of the protonated water dimer. I. Hamiltonian setup and analysis of the ground vibrational state," Journal of Chemical Physics **127**, 184302 (2007).

²C. H. Duong, N. Yang, P. J. Kelleher, M. A. Johnson, R. J. DiRisio, A. B. McCoy, Q. Yu, J. M. Bowman, B. V. Henderson, and K. D. Jordan, "Tagfree and isotopomer-selective vibrational spectroscopy of the cryogenically cooled H₉O₄⁺ cation with two-color, IR-IR double-resonance photoexcitation: Isolating the spectral signature of a single OH group in the hydronium ion core," The Journal of Physical Chemistry A 122, 9275 (2018).

³P. B. Calio, C. Li, and G. A. Voth, "Resolving the structural debate for the hydrated excess proton in water," Journal of the American Chemical Society **143**, 18672 (2021).

⁴C. A. D. Jr., L. M. Streacker, Y. Sun, S. R. Pattenaude, A. A. Hassanali, P. B. Petersen, S. A. Corcelli, and D. Ben-Amotz, "Decomposition of the experimental Raman and infrared spectra of acidic water into proton, special pair, and counterion contributions," Journal of the Physical Chemistry Letters **8**, 5246 (2017).

⁵R. Biswas, W. Carpenter, G. A. Voth, and A. Tokmakoff, "Molecular modeling and assignment of IR spectra of the hydrated excess proton in isotopically dilute water," The Journal of Chemical Physics **145**, 154504 (2016).

⁶W. B. Carpenter, Q. Yu, J. H. Hack, B. Dereka, J. M. Bowman, and A. Tokmakoff, "Decoding the 2D IR spectrum of the aqueous proton with high-level VSCF/VCI calculations," The Journal of Chemical Physics **153**, 124506 (2020).

⁷A. Kundu, F. Dahms, B. P. Fingerhut, E. T. J. Nibbering, E. Pines, , and T. Elsaesser, "Hydrated excess protons in acetonitrile/water mixtures: Solvation species and ultrafast proton motions," Journal of the Physical Chemistry Letters 10, 2287 (2019).

⁸B. M. Auer and J. L. Skinner, "IR and Raman spectra of liquid water: Theory and interpretation," Journal of Chemical Physics 128, 224511 (2008).

⁹O. M. Cracchiolo, D. K. Geremia, S. A. Corcelli, and A. L. Serrano, "Hydrogen bond exchange and Ca²⁺ binding of aqueous N-methylacetamide revealed by 2DIR spectroscopy," The Journal of Physical Chemistry B 124, 6947 (2020).

¹⁰N. Yang, C. H. Duong, P. J. Kelleher, and M. A. Johnson, "Capturing intrinsic site-dependent spectral signatures and lifetimes of isolated OH oscillators in extended water networks," Nature Chemistry 12, 159 (2020).

¹¹C. T. Wolke, J. A. Fournier, L. C. Dzugan, M. R. Fagiani, T. T. Odbadrakh, H. Knorke, K. D. Jordan, A. B. McCoy, K. R. Asmis, and M. A. Johnson, "Spectroscopic snapshots of the proton-transfer mechanism in water," Science 354, 159 (2016).

¹²B. M. Auer and J. L. Skinner, "IR and Raman spectra of liquid water: Theory and interpretation," The Journal of Chemical Physics **127**, 104105 (2007)

¹³A. A. Kananenka and J. L. Skinner, "Fermi resonance in OH-stretch vibrational spectroscopy of liquid water and the water hexamer," Journal of Chemical Physics 148, 244107 (2018).

¹⁴J.-C. Jiang, Y.-S. Wang, H.-C. Chang, S. H. Lin, Y. T. Lee, G. Niedner-Schatteburg, and H.-C. Chang, "Infrared spectra of H⁺(H₂O)₅₋₈ clusters: Evidence for symmetric proton hydration," Journal of the American Chemical Society 122, 1398 (2000).

 15 G. E. Douberly, R. S. Walters, J. Cui, K. D. Jordan, and M. A. Duncan, "Infrared spectroscopy of small protonated water clusters, $\mathrm{H^+(H_2O)}_n$ (n=2-5): Isomers, argon tagging, and deuteration," Journal of Physical Chemistry A **114**, 4570 (2010).

- ¹⁶G. E. Douberly, R. S. Walters, J. Cui, K. D. Jordan, and M. A. Duncan, "Infrared signature of structures associated with the $H^+(H_2O)_n$ (n=6 to 27) clusters," Science **304**, 1137 (2004).
- ¹⁷M. Park, I. Shin, N. J. Singh, and K. S. Kim, "Eigen and Zundel forms of small protonated water clusters: Structures and infrared spectra," Journal of Physical Chemistry A 111, 10692 (2007).
- ¹⁸O. Vendrell, F. Gatti, D. Lauvergnat, and H.-D. Meyer, "Full dimensional (15-dimensional) quantum- dynamical simulation of the protonated water dimer. II. infrared spectrum and vibrational dynamics," Journal of Chemical Physics 127, 184303 (2007).
- ¹⁹J. M. Headrick, E. G. Diken, R. S. Walters, N. I. Hammer, R. A. Christie, J. Cui, E. M. Myshakin, M. A. Duncan, M. A. Johnson, and K. D. Jordan, "Spectral signatures of hydrated proton vibrations in water clusters," Science 308, 1765 (2005).
- ²⁰J. A. Fournier, C. T. Wolke, M. A. Johnson, T. T. Odbadrakh, K. D. Jordan, S. M. Kathmann, and S. S. Xantheas, "Snapshots of proton accommodation at a microscopic water surface: Understanding the vibrational spectral signatures of the charge defect in cryogenically cooled H⁺(H₂O)_{n=2-28} clusters," Journal of Physical Chemistry A 119, 9425 (2015).
- ²¹H. J. Zeng and M. A. Johnson, "Demystifying the diffuse vibrational spectrum of aqueous protons through cold cluster spectroscopy," Annual Review of Physical Chemsitry 72, 667 (2021).
- ²²N. Yang, C. H. Duong, P. J. Kelleher, and M. A. Johnson, "Site-specific vibrational spectral signatures of water molecules in the magic H₃O⁺(H₂O)₂₀ and Cs⁺(H₂O)₂₀ clusters," Proceedings of the National Academy of Sciences 111, 18132 (2014).
- ²³Q. Yu and J. M. Bowman, "Classical, thermostated ring polymer, and quantum VSCF/VCI calculations of IR spectra of H₇O₃⁺ and H₉O₄⁺ (Eigen) and comparison with experiment," The Journal of Physical Chemistry A 123, 1399 (2019).
- ²⁴M. Torrent-Sucarrat and J. M. Anglada, "Anharmonicity and the Eigen-Zundel dilemma in the ir spectrum of the protonated 21 water cluster," Journal of Chemical Theory and Computation 7, 467 (2011).
- ²⁵S. Wallace, L. Huang, C. F. Matta, L. Massa, and I. Bernal, "New structures of hydronium cation clusters," Comptes Rendus Chimie 15, 700 (2012).
- ²⁶M. D. Hanson, J. A. Readnour, A. A. Hassanali, and S. A. Corcelli, "Coupled local-mode approach for the calculation of vibrational spectra: Application to protonated water clusters," Journal of Physical Chemistry Letters 12, 9226 (2021).
- ²⁷J. A. Fournier, C. J. Johnson, C. T. Wolke, G. H. Weddle, A. B. Wolk, and M. A. Johnson, "Vibrational spectral signature of the proton defect in the three-dimensional H⁺(H₂O)₂₁ cluster," Science **344**, 1009 (2014).
- ²⁸Q. Yu and J. M. Bowman, "Tracking hydronium/water stretches in magic H₃O⁺(H₂O)₂₀ clusters through high-level quantum VSCF/VCI calculations," Journal of Physical Chemistry A **124**, 1167 (2013).
- ²⁹C. H. Duong, O. Gorlova, N. Yang, P. J. Kelleher, M. A. Johnson, A. B. McCoy, Q. Yu, and J. M. Bowman, "Disentangling the complex vibrational spectrum of the protonated water trimer, H⁺(H₂O)₃, with two-color IR-IR photodissociation of the bare ion and anharmonic VSCF/VCI theory," Journal of Physical Chemistry Letters 8, 3782 (2017).
- ³⁰C. H. Duong, O. Gorlova, N. Yang, P. J. Kelleher, M. A. Johnson, A. B. Mc-Coy, Q. Yu, and J. M. Bowman, "Communication: VSCF/VCI vibrational spectroscopy of H₇O₃⁺ and H₉O₄⁺ using high-level, many-body potential energy surface and dipole moment surfaces," Journal of Chemical Physics **146**, 121102 (2017).
- ³¹X. Huang, B. J. Braams, and J. M. Bowman, "Ab initio potential energy and dipole moment surfaces for H₅O₂⁺," Journal of Chemical Physics 122, 044308 (2005).
- ³²B. J. Braams and J. M. Bowman, "Permutationally invariant potential energy surfaces in high dimensionality," International Reviews in Physical Chemistry 28, 577 (2009).
- ³³ A. Szabo and N. S. Ostlund, *Modern Quantum Chemistry* (Dover Publications Inc., NY, 1996).
- ³⁴J. S. Mancini and J. M. Bowman, "On-the-fly ab intito calculations of anharmonic vibrational frequencies: Local-monomer theory and application to HCl clusters," Journal of Chemical Physics 139, 164115 (2013).
- ³⁵S. A. Corcelli, C. P. Lawrence, and J. L. Skinner, "Combined electronic structure/molecular dynamics approach for ultrafast infrared spectroscopy

- of dilute HOD in liquid H_2O and D_2O ," Journal of Chemical Physics 120, 8107 (2004).
- ³⁶D. M. de Oliveira, A. J. Bredt, T. C. Miller, S. A. Corcelli, and D. Ben-Amotz, "Spectroscopic and structural characterization of water-shared ion-pairs in aqueous sodium and lithium hydroxide," Journal of the Physical Chemistry B 125, 1439 (2021).
- ³⁷A. A. Kananenka, S. E. Strong, and J. L. Skinner, "Dephasing and decoherence in vibrational and electronic line shapes," Journal of Physical Chemistry B 124, 1531 (2020).
- ³⁸A. R. Leach, *Molecular Modelling: Principles and Applications* (Pearson, U. K., 2001).
- ³⁹A. A. Hassanali, J. Cuny, V. Verdolino, and M. Parrinello, "Aqueous solutions: state of the art in ab initio molecular dynamics," Philosophical Transactions of the Royal Society A 372, 20120482 (2014).
- ⁴⁰C. R. Baiz, B. Błasiak, J. Bredenbeck, M. Cho, J.-H. Choi, S. A. Corcelli, A. G. Dijkstra, C.-J. Feng, S. Garrett-Roe, N.-H. Ge, M. W. D. Hanson-Heine, J. D. Hirst, T. L. C. Jansen, K. Kwac, K. J. Kubarych, C. H. Londergan, H. Maekawa, M. Reppert, S. Saito, S. Roy, J. L. Skinner, G. Stock, J. E. Straub, M. C. Thielges, K. Tominaga, A. Tokmakoff, H. Torii, L. Wang, L. J. Webb, and M. T. Zanni, "Vibrational spectroscopic map, vibrational spectroscopy, and intermolecular interaction," Chemical Reviews 120, 7152 (2020).
- ⁴¹D. T. Colbert and W. H. Miller, "A novel discrete variable representation for quantum mechanical reactive scattering via the S-matrix Kohn method," The Journal of Chemical Physics 96, 1982–1991 (1992).
- ⁴²T. Seideman and W. H. Miller, "Quantum mechanical reaction probabilities via a discrete variable representation-absorbing boundary condition Green's function," The Journal of Chemical Physics 97, 2499 (1992).
- ⁴³E. Wilson, J. Decius, and P. C. Cross, *Molecular Vibrations* (Dover Publications Inc., NY, 1980).
- ⁴⁴J.-H. Choi and M. Cho, "Computational IR spectroscopy of water: OH stretch frequencies, transition dipoles, and intermolecular vibrational coupling constants," Journal of Chemical Physics 138, 174108 (2013).
- ⁴⁵C. Cohen-Tannoudji, B. Diu, and F. Laloe, *Quantum Mechanics* (John Wiley & Sons and Hermann, Paris, France, 1977).
- ⁴⁶G. B. Arfken, H. J. Weber, and F. E. Harris, *Mathematical Methods for Physicists* (Elsevier, MA, 2013).
- ⁴⁷M. D. Hanson, A Coupled Local Mode Method for the Analysis of Molecular Vibrations: Theory and Applications, Ph.D. thesis, University of Notre Dame (2022).
- ⁴⁸D. A. McQuarrie and J. D. Simon, *Physical Chemistry: A Molecular Approach* (University Science Books, CA, 1997).
- ⁴⁹D. A. McQuarrie, *Statistical Mechanics* (University Science Books, CA, 2000).
- ⁵⁰T. Carrington and J. C. Light, "Discrete-variable representations and their utilization," in *Advances in Chemical Physics* (John Wiley & Sons, Hoboken, NJ, 2007) Chap. 4, pp. 263–310.
- ⁵¹A. D. Becke, "Density-functional exchange-energy approximation with correct asymptotic behavior," Physical Reviews A 38, 3098 (1988).
- ⁵²C. Lee, W. Yang, and R. G. Parr, "Development of the Colle-Salvetti correlation-energy formula into a functional of the electron density," Condensed Matter Materials Physics 37, 785 (1988).
- ⁵³J. Vande Vondele, M. Krack, F. Mohamed, M. Parrinello, T. Chassaing, and J. Hutter, "Quickstep: Fast and accurate density functional calculations using a mixed Gaussian and plane waves approach," Computational Physics Communications 167, 103 (2005).
- ⁵⁴S. Goedecker, M. Teter, and J. Hutter, "Separable dual-space Gaussian pseudopotentials," Physical Review B 54, 1703 (1996).
- ⁵⁵G. Bussi, D. Donadio, and M. Parrinello, "Canonical sampling through velocity rescaling," Journal of Chemical Physics 126, 014101 (2007).
- ⁵⁶Y. Shao, Z. Gan, E. Epifanovsky, A. T. B. Gilbert, M. Wormit, J. Kussmann, A. W. Lange, A. Behn, J. Deng, X. Feng, and et al., "Advances in molecular quantum chemistry contained in the Q-Chem 4 program package," Molecular Physics 113, 184 (2015).
- ⁵⁷D. J. Griffiths, *Introduction to Electrodynamics* (Cambridge University Press, 2017, 2017).